This article has been accepted for publication in a future issue of this journal, but has not been fully edited. Content may change prior to final publication. Citation information: DOI 10.1109/TCOMM.2018.2880902, IEEE Transactions on Communications

Distributed Spectrum Sensing for Cognitive Radio Networks Based on the Sphericity Test

Peter J. Smith, *Fellow, IEEE,* Rajitha Senanayake, *Member, IEEE,* Pawel A. Dmochowski, *Senior Member, IEEE,* and Jamie S. Evans, *Senior Member, IEEE*

***Abstract*—We consider spectrum sensing in a cognitive radio network, with arbitrary numbers of primary and secondary users. Based on the sphericity test, we first analyze centralized spectrum sensing where all the data available at the secondary users are combined for the signal detection of primary users. We derive accurate approximations for the false alarm and detection probabilities which are also compared against the approximations already available in literature. Next, we analyze distributed spectrum sensing where only partial data from each secondary user is used in the signal detection of primary users. Two novel techniques namely, the multisample sphericity test and meta analysis, are proposed and analyzed. Instead of sending all the raw data received at the secondary user terminals, in the multisample sphericity test and meta analysis only one or two real numbers are required to be sent to a central processor to make a decision about the presence of primary users. Accurate analytical expressions on the false alarm and detection probabilities are derived and numerical examples are provided to verify their accuracy. Receiver operating characteristic (ROC) curves are also presented to compare the performance of the proposed methods.**

***Index Terms*—**

Cognitive radio, distributed spectrum sensing, sphericity test.

I. Introduction

In view of the radio spectrum's scarcity, it is necessary to find new techniques for its efficient use in wireless communications. In [1], it was revealed that some frequency bands in the radio spectrum are largely unoccupied most of the time. Cognitive radio is a promising technology that can be used to improve radio spectrum utilization, by allowing unlicensed secondary users to share the spectrum resources of licensed primary users [2]–[7]. One principal requirement of this approach is that secondary user transmission does not cause intolerable interference to the primary users. This is achieved by the secondary users' ability to detect the presence of primary users, which is commonly referred to as spectrum sensing. If no primary users are detected, the secondary users are allowed to utilize the primary user's licensed spectrum.

A. Related work and Motivation

Spectrum sensing acts as an important tool in detecting the so called spectrum holes, i.e., idle frequency bands that are temporarily unused by the corresponding primary users, to efficiently deliver secondary user data, while protecting the communication quality of the primary user [8]. It has also been included in the IEEE 802.22 standard, built on cognitive radio techniques [9].

Several spectrum sensing techniques have been proposed in the literature including energy-based detectors [10], [11], eigenvalue-based spectrum sensing techniques [12]–[14], matched-filter based detectors [15] and covariance based spectrum sensing techniques [16], etc. The energy-based detectors are usually simple to implement, but they require knowledge of the effective noise variance. In the present work, we focus on eigenvalue-based spectrum sensing which does not require knowledge of the noise variance and offers remarkably improved performance for specific signal categories. In the literature, many optimal eigenvalue-based spectrum sensing techniques have been proposed and analysed under the assumption of a single active primary user [12]–[14]. However, in cellular systems the existence of multiple, simultaneously transmitting primary users is a prevailing condition and very little is known about performance under the presence of multiple primary users.

For such systems, a novel spectrum sensing algorithm, based on the sphericity test, has been proposed in [17]. The authors use the optimal generalized likelihood ratio test (GLRT) paradigm and simulate the false alarm and detection probabilities. However, no analytical derivation relating to the performance measures was presented. In [18], the authors adopt the same model as in [17] and derive analytical formulae to approximate the false alarm and detection probabilities in the presence of multiple primary users. The approximation was derived by matching the moments of test statistics to a Beta distribution. For the special case of only two secondary users the approximations in [18] reduce to the exact performance measures. In [19] and [20], the authors derive exact expressions for the moments of the GLRT statistic, and show that the normalized GLRT statistic converges in distribution to a Gaussian random variable when the number of antennas and observations grow large at the same rate.

While the optimal GLRT technique considered in [17]–[20] exhibits high detection performance, it requires a central

Peter J. Smith and Pawel A. Dmochowski are with Victoria University of Wellington, New Zealand (email: peter.smith@ecs.vuw.ac.nz, pawel.dmochowski@ecs.vuw.ac.nz).

Rajitha Senanayake and Jamie S. Evans are with The University of Melbourne, Australia (email: rajitha.senanayake@unimelb.edu.au, jse@unimelb.edu.au).

Manuscript received June 21, 2018; revised August 20, 2018; accepted November 5, 2018. The review of this paper was coordinated by Dr. Kyeong Jin Kim.

This work is supported in part by the Australian Research Council (ARC) through the Discovery Early Career Researcher (DECRA) Award DE180100501 and the Discovery Project (DP) DP140101050.

This article has been accepted for publication in a future issue of this journal, but has not been fully edited. Content may change prior to final publication. Citation information: DOI 10.1109/TCOMM.2018.2880902, IEEE Transactions on Communications

processor that gathers and processes the raw data received by all the secondary user terminals. This centralized architecture limits the applicability of the GLRT technique to large networks due to the resulting communication and computation burden. In order to overcome this problem, we are motivated to consider more decentralized spectrum sensing techniques that require only partial information to be exchanged between the secondary users and the central processor. More specifically, we consider cases where the secondary users process the data locally at the terminal, and share the processed data with the central processor to make the final decision.

B. Contributions

In this paper, we consider a general cognitive radio system with an arbitrary number of primary and secondary user terminals. Based on the sphericity test and the GLRT statistic we investigate the detection performance of centralized and decentralized spectrum sensing. Our novel contributions are detailed as follows:

- Under centralized spectrum sensing we derive easy-to-evaluate closed-form approximations for the false alarm and the detection probabilities. Based on numerical examples, we illustrate the accuracy of our approximations and compare them against the analytical approximations in [18] and [20].
- Under distributed spectrum sensing we propose two novel techniques, namely, the multisample sphericity test and meta analysis. In the multisample sphericity test each secondary user calculates and sends only two real numbers, specifically, the trace and the determinant of the sample covariance matrix, to detect the primary user signal. Under this scheme, we derive easy-to-evaluate, closed-form approximations for the false alarm and detection probabilities when the secondary users are subject to equal or unequal noise variances.
- In meta analysis each secondary user is required to calculate and send only one real number, i.e., the extreme probability value, more commonly known as the p-value, of the current test statistic. Under this technique also, we derive an easy-to-evaluate, closed-form approximation for the false alarm probability.
- Furthermore, we compare the performance of the novel techniques with other simple binary fusion methods, where each secondary user terminal makes a binary decision about the presence of primary users and all the decisions are simply combined through binary AND or OR operation at the central processor. Under binary fusion techniques also, we conduct a rigorous theoretical analysis by deriving closed-form approximations for the test statistics distributions under both hypothesis.
- We present extensive numerical examples to illustrate the accuracy of our results. Using the receiver operating characteristics (ROC), curves we compare the performance of the proposed techniques. We observe that both the multisample sphericity test and meta analysis have similar performance even though meta analysis requires only half the amount of information sent to the central processor.

The rest of the paper is organized as follows. In Section II we present the system model and outline the sphericity test based centralized test statistics. The theoretical analyses on deriving the false alarm and detection probabilities are also presented. In Section III, we present the novel techniques of multisample sphericity test and meta analysis, and analyze the false alarm probability and detection probabilities. We also compare the performance of different distributed spectrum sensing techniques based on ROC curves and present numerical examples. The paper is concluded in Section IV.

II. Centralized spectrum sensing

We consider a standard wireless communications system with P primary user terminals and M secondary user terminals. The secondary user terminals are tasked with cooperatively determining the presence of primary users and the secondary user terminal m is equipped with Q_m antennas such that, $K = \sum_{m=1}^{M} Q_m$. In this system, each secondary user terminal is connected to a central processor[1], that cooperatively detects the presence of primary users. The amount of information exchanged to the central processor could vary depending on the type of spectrum sensing technique used. This detection problem can be formulated as a binary hypothesis test, where the null hypothesis, $\mathcal{H}_0$, denotes the absence of primary users and the non-null hypothesis, $\mathcal{H}_1$, denotes the presence of primary users. Under centralized spectrum sensing we assume that all the signals received at the secondary user terminals are available at the central processor. As such, the n-th sample vector, $\mathbf{x}_n$, received at the central processor can be modeled as

$$\begin{aligned} \mathcal{H}_0: &\quad \mathbf{x}_n = \mathbf{w}_n && \text{no primary users present} \\ \mathcal{H}_1: &\quad \mathbf{x}_n = \mathbf{H}\mathbf{s} + \mathbf{w}_n && \text{primary users present,} \end{aligned} \tag{1}$$

where $\mathbf{s} = [s_1, s_2, \ldots, s_P]^T$ is the $P \times 1$ data vector, which contains the zero mean transmitted symbols from the P primary users, $\mathbf{w}_n$ is the $K \times 1$ additive white Gaussian noise vector at the n-th sample with $\mathbb{E}[\mathbf{w}_n \mathbf{w}_n^\dagger] = \sigma^2 \mathbf{I}_K$ and, $\mathbf{H} = [\mathbf{h}_1, \mathbf{h}_2, \ldots, \mathbf{h}_P]$ is the $K \times P$ channel matrix between the P primary users and K receive antennas. We collect N independent and identically distributed sample vectors such that the observed received signal matrix is $\mathbf{X} = [\mathbf{x}_1, \mathbf{x}_2, \ldots, \mathbf{x}_N]$. Similar to [18], we assume that the channel $\mathbf{H}$ remains constant during this time. Note that unless otherwise specified, the results in this paper do not assume a specific distribution for $\mathbf{H}$. We also assume that the primary users signal follows an independent and identically distributed zero mean Gaussian distribution and is uncorrelated with the noise.

A. Sphericity Test

Let us define the sample covariance matrix $\mathbf{R} = \mathbf{X}\mathbf{X}^\dagger$ such that when no primary users are present $\mathbf{R}$ follows an uncorrelated complex Wishart distribution with population covariance matrix

$$\mathbf{\Sigma} = \frac{\mathbb{E}[\mathbf{X}\mathbf{X}^\dagger]}{N} = \sigma^2 \mathbf{I}_K. \tag{2}$$

[1]One of the secondary user terminals could be selected as the central processor.

This article has been accepted for publication in a future issue of this journal, but has not been fully edited. Content may change prior to final publication. Citation information: DOI 10.1109/TCOMM.2018.2880902, IEEE Transactions on Communications

When primary users are present, for a given $\mathbf{H}$, $\mathbf{R}$ follows a correlated complex Wishart distribution with population covariance matrix

$$\mathbf{\Sigma} = \sum_{i=1}^{P} \gamma_i \mathbf{h}_i \mathbf{h}_i^{\dagger} + \sigma^2 \mathbf{I}_K, \tag{3}$$

where $\gamma_i = \mathbb{E}[s_i s_i^{\dagger}]$ defines the transmission power of the i-th primary user. Thus, the hypothesis testing in (1) can be rearranged to test the structure of the population covariance matrix $\mathbf{\Sigma}$ as

$$\begin{aligned} \mathcal{H}_0 : \quad & \mathbf{\Sigma} = \sigma^2 \mathbf{I}_K && \text{no primary users present} \\ \mathcal{H}_1 : \quad & \mathbf{\Sigma} \succ \sigma^2 \mathbf{I}_K && \text{primary users present,} \end{aligned} \tag{4}$$

where $\mathbf{A} \succ \mathbf{B}$ denotes that $\mathbf{A} - \mathbf{B}$ is a positive definite matrix. Note that no a priori knowledge on $\mathbf{H}$, P and σ^2 is assumed at the secondary user terminals. The most critical information for the secondary user is whether or not there are active primary users and the number of active users is not relevant. As such, we reject $\mathcal{H}_0$ if we have reason to believe that $\mathbf{\Sigma}$ departs from the spherical structure of $\mathbf{\Sigma} = \sigma^2 \mathbf{I}_K$, which is the well-known sphericity test [21], [22].

Different test criteria can be considered for the detection problem in (4). In this paper, we consider detectors of the Neyman-Pearson type, which involves comparing the generalized likelihood ratio to a user-designed detection threshold [23]. The generalized likelihood ratio used for determining $\mathcal{H}_0$ or $\mathcal{H}_1$ in (4) can be written as

$$\mathcal{L} = \frac{\sup_{\sigma^2 \in \mathbb{R}^+} L(\mathbf{X}|\sigma^2 \mathbf{I}_K)}{\sup_{\mathbf{\Sigma} \succ 0} L(\mathbf{X}|\mathbf{\Sigma})}, \tag{5}$$

where $L(\mathbf{X}|\sigma^2 \mathbf{I}_K)$ is the likelihood function of the observation matrix under hypothesis $\mathcal{H}_0$ and $L(\mathbf{X}|\mathbf{\Sigma})$ is the likelihood function of the observation matrix under hypothesis $\mathcal{H}_1$. Maximizing these likelihoods over the unknown parameters, i.e., finding the maximum likelihood estimates of σ^2 under $\mathcal{H}_0$, and of $\sigma^2, \gamma_1, \gamma_2, \ldots, \gamma_P$ and $\mathbf{H}$ under $\mathcal{H}_1$, results in the GLRT statistic [24]

$$\text{TS} = \frac{|\mathbf{R}|}{\left(\frac{1}{K}\text{tr}(\mathbf{R})\right)^K}. \tag{6}$$

More details on the derivation of TS can be found in [18], [24]. Now, to determine $\mathcal{H}_0$ or $\mathcal{H}_1$ admits

$$\text{TS} \underset{\mathcal{H}_1}{\overset{\mathcal{H}_0}{\gtrless}} \zeta, \tag{7}$$

where ζ is a user-specified detection threshold. Thus, the central processor calculates TS and declares that the primary user signals are present if TS $< \zeta$, while no primary user signals are believed to be present if TS $> \zeta$.

B. Performance Measures

We consider two performance measures for the sphericity test based detection, namely, the false alarm probability denoted by P_{fa} and the detection probability denoted by P_d. In the following, we present the analytical results of those performance measures in closed-form expressions. We note that under centralized spectrum sensing approximate expressions for the false alarm probability and detection probability are derived in [18], [20]. In [18], the test statistic is approximated by a beta variable based on the moments of the distributions involved. In [20], the inverse of the test statistic is approximated using a Gaussian random variable. In the present paper, we derive alternative approximations for P_{fa} and P_{d} that are more accurate and yet easy-to-evaluate. In addition to the simplicity, our results are based on chi-squared (for P_{fa}) and normal (for P_{d}) approximations, which have a rigorous mathematical basis in asymptotic expansions as shown in [24, pg. 436] and [22, pg. 351], respectively. Numerical examples are presented comparing our results with the results in [18], [20].

1) Probability of false alarm: The false alarm probability is the probability of wrongly declaring $\mathcal{H}_1$, i.e., $\mathcal{H}_1$ is chosen given that $\mathcal{H}_0$ is the true hypothesis. It can be defined as

$$P_{\text{fa}} = \Pr[\text{TS}_{\mathcal{H}_0} \leq \zeta], \tag{8}$$

where $\text{TS}_{\mathcal{H}_0}$ is TS defined under hypothesis $\mathcal{H}_0$. From (8), note that P_{fa} is the CDF of $\text{TS}_{\mathcal{H}_0}$, evaluated at ζ which can be denoted by $F_{\text{TS}_{\mathcal{H}_0}}(\zeta)$. The threshold ζ should be carefully chosen such that P_{fa} is small and it can be calculated by numerically inverting $F_{\text{TS}_{\mathcal{H}_0}}(\zeta)$, i.e.,

$$\zeta = F^{-1}_{\text{TS}_{\mathcal{H}_0}}(P_{\text{fa}}). \tag{9}$$

In order to analyse P_{fa}, first we use the result in [18, eq. (35)] to find the exact moments of the N-th power of $\text{TS}_{\mathcal{H}_0}$, i.e., $\text{TS}^N_{\mathcal{H}_0}$, as

$$\text{E}[\text{TS}^{nN}_{\mathcal{H}_0}] = K^{Kn} \frac{\Gamma(NK)}{\Gamma(NK + nNK)} \prod_{k=1}^{K} \frac{\Gamma(N + nN - k + 1)}{\Gamma(N - k + 1)}, \tag{10}$$

where n denotes the n-th moment and $\Gamma(\cdot)$ denotes the gamma function [25, eq. (8.310)]. Next, we proceed to compare these moments with [24, Section 8.5.1, eq. (1)]. We observe that the expression in [24, Section 8.5.1, eq. (1)] reduces to (10) when the constant $K = \Gamma(NK)\left(\prod_{k=1}^{K}\Gamma(N+1-k)\right)^{-1}$, $b = 1$, $a = K$, $y_1 = NK$, $x_k = N \;\forall\; k \in \{1, 2, \ldots, a\}$, $\eta_1 = 0$ and $\{-\xi_1, -\xi_2, \ldots, -\xi_a\} = \{0, \ldots, K\}$. Hence we can directly apply the general theory of asymptotic expansions in [24, Section 8.5.1] to derive an approximation to the CDF of $-2N\rho \ln(\text{TS}_{\mathcal{H}_0})$ under the null hypothesis as

$$\Pr[-2\rho \ln(\text{TS}_{\mathcal{H}_0}) \leq x] \approx \Pr[\chi^2_f \leq x], \tag{11}$$

where $f = K^2 - 1$, $\rho = N - \frac{1+2K^2}{6K}$, and χ^2_f denotes a chi-squared distribution with f degrees of freedom. Note that the full expression for the CDF of $-2N\rho \ln(\text{TS}_{\mathcal{H}_0})$ in [24] contains additional correction terms written in-terms of higher order chi-squared distributions. For simplicity, we ignore these correction terms and approximate $\Pr[-2N\rho \ln(\text{TS}_{\mathcal{H}_0}) \leq x]$ by the chi-squared distribution in (11). We also note that this results can be obtained by using [26], [27]. Following simple mathematical manipulations (11) can be expressed as

$$\Pr\left[\text{TS}_{\mathcal{H}_0} \geq \exp\left(-\frac{x}{2N\rho}\right)\right] \approx \Pr[\chi^2_f \leq x]. \tag{12}$$

This article has been accepted for publication in a future issue of this journal, but has not been fully edited. Content may change prior to final publication. Citation information: DOI 10.1109/TCOMM.2018.2880902, IEEE Transactions on Communications

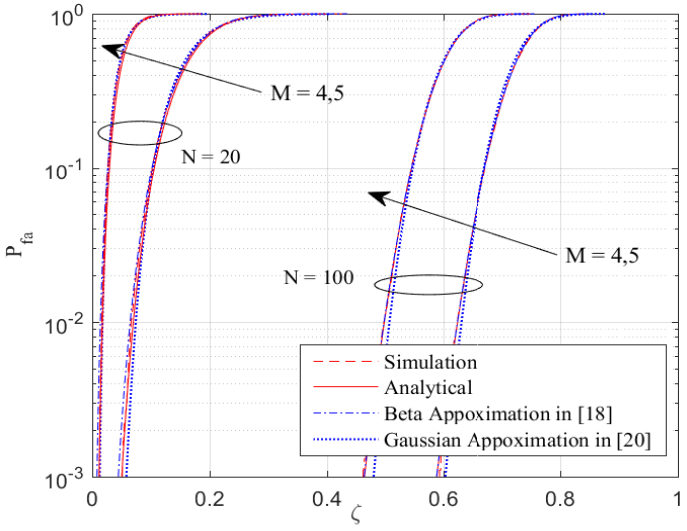

Fig. 1. Probability of false alarm vs the detection threshold for centralized spectrum sensing.

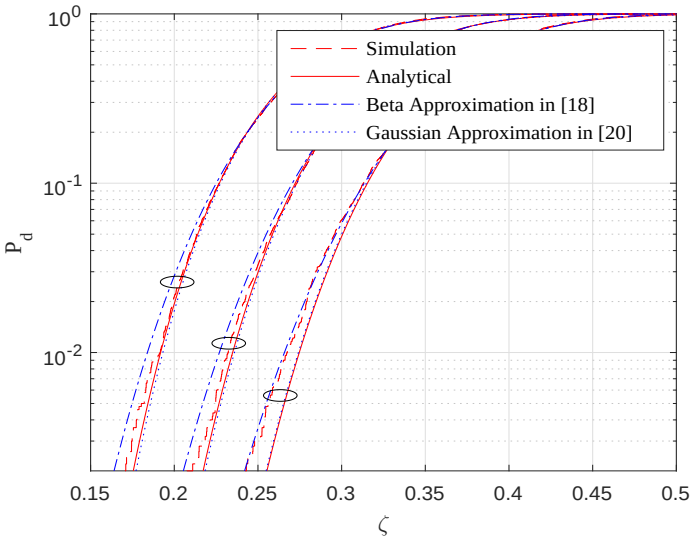

Fig. 2. Probability of detection vs the detection threshold for centralized spectrum sensing.

Hence, we can derive an approximation for the CDF of $\text{TS}_{\mathcal{H}_0}$ as

$$\Pr[\text{TS}_{\mathcal{H}_0} \leq x] \approx 1 - \Pr[\chi_f^2 \leq -2N\rho \ln(x)]. \quad (13)$$

Thus, P_{fa} for centralized spectrum sensing can be approximated as

$$P_{\text{fa}} \approx 1 - \Pr[\chi_f^2 \leq -2N\rho \ln(\zeta)]. \quad (14)$$

Comparing (14) with [18, eq. (17)] and [20, eq. (11)] we notice that our results has a much simpler form and is very easy to evaluate.

Fig. 1 plots the P_{fa} versus the detection threshold ζ for different numbers of secondary user terminals, by setting $M = 4$ and 5. The secondary use terminals are allocated $Q_m = 2$ antennas each. We also change the number of observations, by setting $N = 20$ and 100. For each simulation trial, the noise components are drawn from an independent complex Gaussian distribution. The simulation curves are generated based on Monte-Carlo simulation, while the analytical curves are generated using the approximation in (14). The figure illustrates extremely close agreement between the analytical approximation and the simulation curves. For a given detection threshold, an increase in M results in an increase in P_{fa}. We also compare these results with the beta and Gaussian approximations in [18] and [20][2], respectively. We observe that when compared to the accuracy of our analytical approximation, the beta approximation in [18, eq. (17)] is slightly loose in the lower tail when $N = 20$ and, the Gaussian approximation in [20, eq. (11)] is slightly loose in the lower tail when $N = 100$.

[2]In Fig. 1 we plot the Gaussian approximation in [20], without the correction terms. We agree that adding the correction terms will make the approximation more accurate, but the complexity of the approximation increases as it requires the calculation of the third and the fourth central moments of X. Therefore, to keep the complexity comparable with (14) and [18, eq. (17)] we ignore the correction terms in [20, eq. (11)].

2) Probability of detection: The detection probability is the probability of declaring correctly $\mathcal{H}_1$, i.e., $\mathcal{H}_1$ is chosen given that $\mathcal{H}_1$ is the true hypothesis. It can be defined as

$$\begin{aligned} P_{\text{d}} &= \Pr[\text{TS}_{\mathcal{H}_1} \leq \zeta] \\ &= F_{\text{TS}_{\mathcal{H}_1}}(\zeta), \end{aligned} \quad (15)$$

where $\text{TS}_{\mathcal{H}_1}$ is TS defined under hypothesis $\mathcal{H}_1$ and $F_{\text{TS}_{\mathcal{H}_1}}(\zeta)$ is the CDF of $\text{TS}_{\mathcal{H}_1}$ evaluated at ζ.

In order to analyse P_{d}, we first use [22, Theorem 8.3.9] to learn that under $\mathcal{H}_1$, the distribution of the variable $\ln(\text{TS}_{\mathcal{H}_1})$ is closely Gaussian. This is also confirmed by the Monte-Carlo simulations which showed that the empirical distribution of $\ln(\text{TS}_{\mathcal{H}_1})$ approaches a Gaussian as the number of observations grows large. Motivated by these observations we proceed to approximate the CDF of $\text{TS}_{\mathcal{H}_1}$ using a Gaussian distribution as

$$\Pr[\text{TS}_{\mathcal{H}_1} \leq x] \approx \Pr[Z \leq \ln(x)], \quad (16)$$

where $Z \sim \mathcal{N}(\mu, \nu^2)$, $\mu = \frac{K}{2}\ln(m_2) - 2K\ln(m_1)$ and $\nu^2 = K^2\ln(m_2) - 2K^2\ln(m_1)$ denote the mean and the variance of the Gaussian distribution. The terms m_1 and m_2 denote the first and the second moments of $\text{TS}_{\mathcal{H}_1}^{-1/K}$, respectively, and are given by (17) and (18) at the top of the next page, with $\sigma^2 < \lambda_1 \leq \lambda_2 \leq \ldots \leq \lambda_K < \infty$ denoting the eigenvalues of $\mathbf{H}\mathbf{H}^{\dagger} + \sigma^2\mathbf{I}_K$. A detailed proof of (16) is given in Appendix A.

Based on (16), P_{d} for centralized spectrum sensing can be approximated as

$$P_{\text{d}} \approx \Pr[Z \leq \ln(\zeta)]. \quad (19)$$

Comparing (19) with [18, eq. (25)] and [20, eq. (11)] we notice that our result has a much simpler form and is trivial evaluate.

Fig. 2 plots P_{d} versus the detection threshold ζ for a network with $P = 3$ primary users, $M = 5$ and $N = 100$. The secondary user terminals are allocated $Q_m = 2$ antennas each.

This article has been accepted for publication in a future issue of this journal, but has not been fully edited. Content may change prior to final publication. Citation information: DOI 10.1109/TCOMM.2018.2880902, IEEE Transactions on Communications

$$m_1 = \left(\frac{NK-1}{K^2}\right)\prod_{k=1}^{K}\lambda_k^{-1/K}\prod_{j=0}^{K-1}\frac{\Gamma(N-K-1/K+1+j)}{\Gamma(N-K+1+j)}\sum_{i=1}^{K}\lambda_i, \tag{17}$$

$$m_2 = \left(\frac{NK-2}{K^3}\right)\prod_{k=1}^{K}\lambda_k^{-2/K}\prod_{j=0}^{K-1}\frac{\Gamma(N-K-2/K+1+j)}{\Gamma(N-K+1+j)}\left[\sum_{i=1}^{K}\lambda_i+\left(N-\frac{2}{K}\right)\left(\sum_{i=1}^{K}\lambda_i\right)^2\right], \tag{18}$$

We fix the transmit power values as $\gamma_1 = \gamma_2 = \gamma_3 = -10$ dB and plot the detection probability for three different channel realizations. The simulation curves are generated based on Monte-Carlo simulation, while the analytical curves are generated using the approximation in (19). The figure illustrates close agreement between the approximation and the simulation curves. We also compare this results with the beta and Gaussian approximations in [18] and [20]. We observe that the approximation in [20] and our result have very close performance as the distributions of both $1/\text{TS}_{\mathcal{H}_1}$ and $\ln(\text{TS}_{\mathcal{H}_1})$ are closely Gaussian. Observing the lower tail of the plots, we also understand that the accuracy of each approximation depends on the random channel realization that is selected.

III. Decentralized spectrum sensing

In this section, we consider decentralized spectrum sensing. Under the centralized spectrum sensing we assume that all the signals received at secondary user terminals are received at the central processor. However, centralized spectrum sensing is not very suitable for practical implementations of cognitive radio networks. This is because calculating TS requires the sharing of all raw data received at the M secondary user terminals with the central processor, producing considerable network overhead. Based on the sphericity test and the GLRT statistic, in the following we analyze two new spectrum sensing techniques namely, the multisample sphericity test and meta analysis that require the exchange of only partial information, with the central processor. Furthermore, we investigate the simple binary fusion technique and compare the performance.

We consider the same system model as described in Section II. Under this distributed setup we define the two hypotheses, $\mathcal{H}_0$ and $\mathcal{H}_1$, for sphericity as

$$\begin{aligned}\mathcal{H}_0:\ &\mathbf{\Sigma}_m = \sigma^2\mathbf{I}_{Q_m} \quad \text{for all } m \in \{1,2,\ldots,M\},\\ \mathcal{H}_1:\ &\mathbf{\Sigma}_m \succ \sigma^2\mathbf{I}_{Q_m} \quad \text{for at least one } m \in \{1,2,\ldots,M\},\end{aligned} \tag{20}$$

where $\mathbf{\Sigma}_m = \mathbb{E}[\mathbf{X}_m\mathbf{X}_m^\dagger]/N$ is the population covariance matrix with $\mathbf{X}_m$ denoting the $Q_m \times N$ observed data matrix at the secondary user terminal m.

A. Multisample sphericity test

In this subsection we present the first novel distributed spectrum sensing technique named, the multisample sphericity test. Based on the distributed setup, the generalized likelihood ratio for determining $\mathcal{H}_0$ or $\mathcal{H}_1$ defined in (20) can be written as

$$\tilde{\mathcal{L}} = \frac{\sup_{\sigma^2\in\mathbb{R}^+}\tilde{L}(\mathbf{X}_1,\mathbf{X}_2,\ldots,\mathbf{X}_M|\sigma^2\mathbf{I}_{Q_1},\ldots,\sigma^2\mathbf{I}_{Q_M})}{\sup_{\mathbf{\Sigma}_1\succ 0,\ldots,\mathbf{\Sigma}_M\succ 0}\tilde{L}(\mathbf{X}_1,\mathbf{X}_2,\ldots,\mathbf{X}_M|\mathbf{\Sigma}_1,\ldots,\mathbf{\Sigma}_M)}, \tag{21}$$

where $\tilde{L}(\mathbf{X}_1,\mathbf{X}_2,\ldots,\mathbf{X}_M|\sigma^2\mathbf{I}_{Q_1},\ldots,\sigma^2\mathbf{I}_{Q_M})$ is the likelihood function of the observation matrices under hypothesis $\mathcal{H}_0$ and $\tilde{L}(\mathbf{X}_1,\mathbf{X}_2,\ldots,\mathbf{X}_M|\mathbf{\Sigma}_1,\ldots,\mathbf{\Sigma}_M)$ is the likelihood function of the observation matrices under hypothesis $\mathcal{H}_1$. Following the derivation methodology in [22, Theorem 8.3.2] and maximizing these likelihoods over the unknown parameters, the modified GLRT statistic for testing the above hypothesis can be obtained as

$$\text{MSTS} = \frac{\prod_{m=1}^{M}|\mathbf{R}_m|}{\left(\frac{1}{K}\sum_{m=1}^{M}\text{tr}(\mathbf{R}_m)\right)^K}, \tag{22}$$

where $\mathbf{R}_m = \mathbf{X}_m\mathbf{X}_m^\dagger$ is the sample covariance matrix at the secondary user terminal m. Note that the MSTS in (22) reduces to a similar form to TS in (6) when $M = 1$. Thus, instead of sending the whole matrix $\mathbf{X}_m$, which is the case with the centralized spectrum sensing, the multisample sphericity test requires the secondary user terminal m to calculate $|\mathbf{R}_m|$ and $\text{tr}(\mathbf{R}_m)$ and share with the central processor the two real numbers. The central processor collects all matrix determinants and traces from the M secondary user terminals and calculates the global MSTS according to (22). We determine $\mathcal{H}_0$ or $\mathcal{H}_1$ in the multisample sphericity test as

$$\text{MSTS} \underset{\mathcal{H}_1}{\overset{\mathcal{H}_0}{\gtrless}} \zeta. \tag{23}$$

In order to analyse the performance of the multisample sphericity test, we next proceed to derive an analytical expression for P_{fa} and P_{d} based on (22).

1) Probability of false alarm: Based on [18], we first write the exact n-th moment of the N-th power of MSTS under $\mathcal{H}_0$ as

$$\text{E}[(\text{MSTS}_{\mathcal{H}_0})^{Nn}] = \frac{K^{nNK}\Gamma(NK)}{\Gamma(NK+nNK)}\prod_{m=1}^{M}\prod_{q=1}^{Q_m}\frac{\Gamma(N+nN+1-q)}{\Gamma(N+1-q)}, \tag{24}$$

where $\text{MSTS}_{\mathcal{H}_0}$ denotes the MSTS under $\mathcal{H}_0$, Similar to Section II-B1, next we proceed to compare (24) with [24, Section 8.5.1, eq. (1)]. We observe that the expression in [24, Section 8.5.1, eq. (1)] reduces to (24) when the constant $K = \Gamma(NK)\left(\prod_{m=1}^{M}\prod_{q=1}^{Q_m}\Gamma(N+1-q)\right)^{-1}$,

This article has been accepted for publication in a future issue of this journal, but has not been fully edited. Content may change prior to final publication. Citation information: DOI 10.1109/TCOMM.2018.2880902, IEEE Transactions on Communications

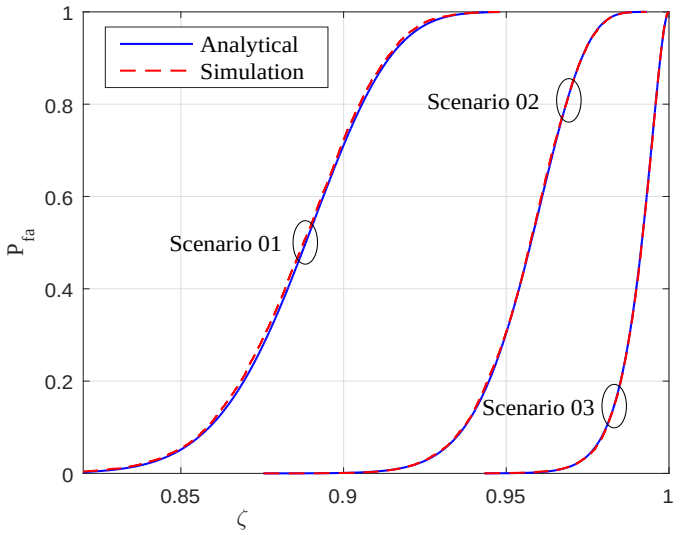

Fig. 3. Probability of false alarm vs the detection threshold for scenario 01, 02 and 03 with N = 200, $M = 5$.

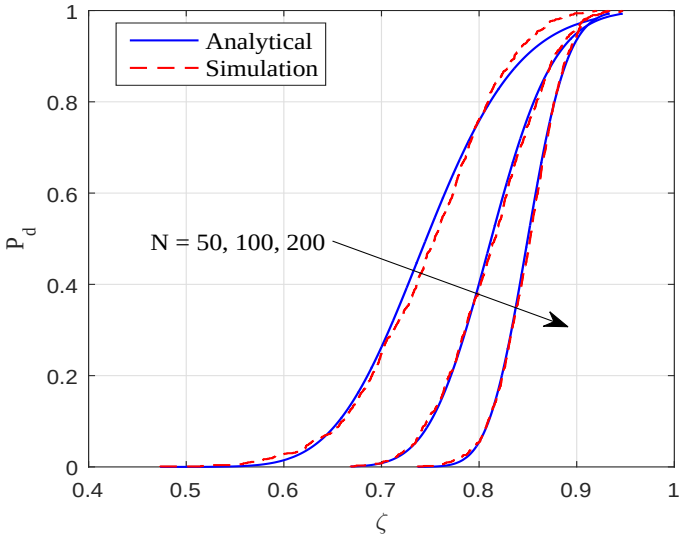

Fig. 4. Probability of detection vs the detection threshold for N = 50, 100 and 200, with $M = 2$ and $Q_m = 3$.

$b = 1$, $a = K$, $y_1 = NK$, $x_k = N \ \forall \ k \in \{1, 2, \ldots, a\}$, $\eta_1 = 0$ and $\{-\xi_1, -\xi_2, \ldots, -\xi_a\} = \{0, \ldots, Q_1 - 1, 0, \ldots, Q_2 - 1, \ldots, 0, \ldots, Q_M - 1\}$. Thus, we follow the expansion method in [24, Section 8.5.1] and derive an approximation to the CDF of $-2\tilde{\rho}\ln(\text{MSTS}_{\mathcal{H}_0})$ under the null hypothesis as

$$\Pr[-2\tilde{\rho}\ln(\text{MSTS}_{\mathcal{H}_0}) \leq x] \approx \Pr[\chi^2_{\tilde{f}} \leq x], \tag{25}$$

where $\tilde{f} = \sum_{m=1}^{M} Q_m^2 - 1$, $\tilde{\rho} = N - \frac{1+K^2-2K\sum_{m=1}^{M} Q_m^3}{6K(1-\sum_{m=1}^{M} Q_m^2)}$. Following simple mathematical manipulations an approximation for the CDF of MSTS can be derived as

$$\Pr[\text{MSTS}_{\mathcal{H}_0} \leq x] \approx 1 - \Pr[\chi^2_{\tilde{f}} \leq -2\tilde{\rho}\ln(x)]. \tag{26}$$

Thus, P_{fa} for the multisample sphericity test can be approximated as

$$P_{\text{fa}} \approx 1 - \Pr[\chi^2_{\tilde{f}} \leq -2\tilde{\rho}\ln(\zeta)]. \tag{27}$$

Fig. 3 plots P_{fa} versus the detection threshold ζ for different number of antennas at each secondary user terminal. For fixed $M = 5$, $N = 200$, we consider the following three scenarios. In scenario 01, $Q_1 = 3$, $Q_2 = 1$ $Q_3 = 2$, $Q_4 = 4$ and $Q_5 = 2$. In scenario 02, $Q_1 = 2$, $Q_2 = 1$ $Q_3 = 1$, $Q_4 = 3$ and $Q_5 = 2$, and in scenario 03, $Q_m = 1, \forall m \in \{1, 2, \ldots 5\}$. As such, the root mean square (RMS) value of the number of antennas is 2.6, 1.67 and 1, respectively. As observed in the conference vesion of this paper [28], the figure illustrates that the approximation is very accurate for all three scenarios and for a given detection threshold the P_{fa} increases with the increasing RMS value of Q_m.

2) Probability of detection: We follow a similar approach to Section II-B2 and approximate the distribution of $\ln(\text{MSTS}_{\mathcal{H}_1})$, where $\text{MSTS}_{\mathcal{H}_1}$ denotes MSTS under $\mathcal{H}_1$, by a Gaussian distribution with mean $\tilde{\mu}$ and variance $\tilde{\nu}^2$. Let us first define a new random variable $\tilde{X}$ such that

$$\tilde{X} \approx \ln\left(\frac{1}{\text{MSTS}_{\mathcal{H}_1}}\right), \tag{28}$$

and $\tilde{X} \sim \mathcal{N}(-\tilde{\mu}, \tilde{\nu}^2)$. Based on (28), we can approximate the first and the second moments of $\text{MSTS}_{\mathcal{H}_1}$ as

$$\tilde{m}_1 = \text{E}\left[\left(\frac{1}{\text{MSTS}_{\mathcal{H}_1}}\right)\right] \approx \text{E}[e^X] = e^{-\tilde{\mu}+\frac{\tilde{\nu}^2}{2}}, \tag{29}$$

$$\tilde{m}_2 = \text{E}\left[\left(\frac{1}{\text{MSTS}_{\mathcal{H}_1}}\right)^2\right] \approx \text{E}[e^{2X}] = e^{-2\tilde{\mu}+2\tilde{\nu}^2}, \tag{30}$$

where (29) and (30) are derived using the moment generating function. Next, we take the ratio between (29) and (30) and do some mathematical manipulations to derive approximate expressions for $\tilde{\mu}$ and $\tilde{\nu}^2$ in terms of $\tilde{m}_1$ and $\tilde{m}_2$ as

$$\tilde{\mu} \approx \ln(\tilde{m}_2) - 2\ln(\tilde{m}_1), \tag{31}$$

$$\tilde{\nu}^2 \approx \frac{1}{2}\ln(\tilde{m}_2) - 2\ln(\tilde{m}_1). \tag{32}$$

We derive the exact expressions for $\tilde{m}_1$ and $\tilde{m}_2$ in Appendix C and the resultant closed-form expressions can be found in (81) and (84), respectively.

Thus, the CDF Of $\ln(\text{MSTS}_{\mathcal{H}_1})$ can be approximated by

$$\Pr[\ln(\text{MSTS}_{\mathcal{H}_1}) \leq x] \approx \Pr[\tilde{Z} \leq x], \tag{33}$$

where $\tilde{Z} \sim \mathcal{N}(\tilde{\mu}, \tilde{\nu}^2)$, $\tilde{\mu}$ and $\tilde{\nu}$ can be approximated by substituting (81) and (84) into (31) and (32), respectively. Based on (33), P_{d} for decentralized spectrum sensing with multisample sphericity test can be approximated as

$$P_{\text{d}} \approx \Pr[\tilde{Z} \leq \ln(\zeta)]. \tag{34}$$

Fig. 4 plots P_d versus the detection threshold ζ for different number of sample sizes N. Here we select an example where

This article has been accepted for publication in a future issue of this journal, but has not been fully edited. Content may change prior to final publication. Citation information: DOI 10.1109/TCOMM.2018.2880902, IEEE Transactions on Communications

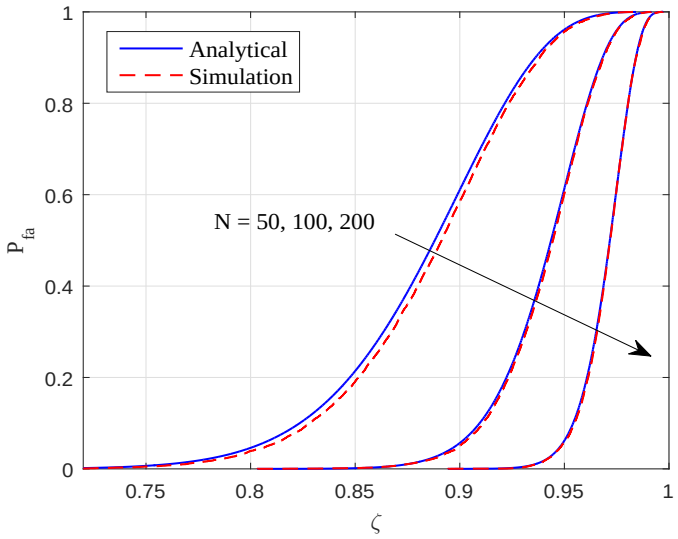

Fig. 5. Probability of false alarm vs the detection threshold for N = 50, 100, and 200 with $M = 4$ and $Q_m = 2$.

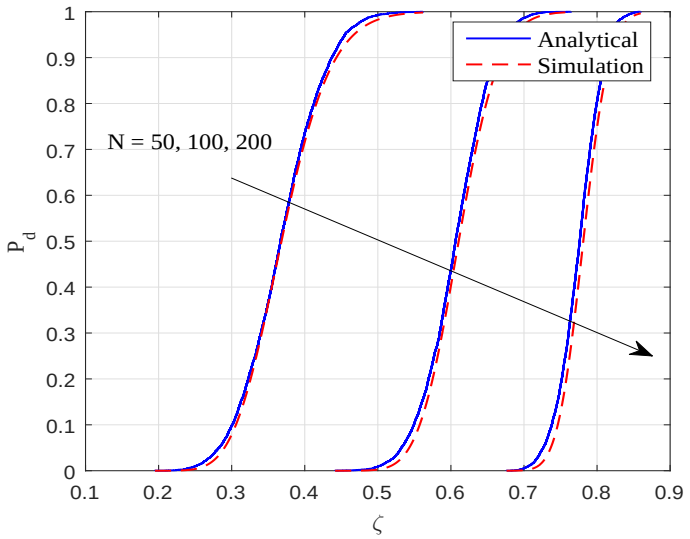

Fig. 6. Probability of detection vs the detection threshold for N = 50, 100, and 200 with $M = 4$ and $Q_m = 5$.

$P = 2$, $M = 2$, $Q_1 = Q_2 = 3$ and examine P_d for $N = 50, 100$ and 200. We fix the transmit power values to $\gamma_1 = \gamma_2 = -10$ dB. The simulation curves are generated using Monte-Carlo simulations while the analytical curves are generated using the approximation in (34). As the Gaussian approximation is large sample based, we expect the approximation to be more accurate when N is large. This is clearly illustrated by the close agreement between the approximation and the simulation curves, especially when $N = 100$ and 200.

3) Multisample sphericity test with unequal noise variance: Under the distributed hypothesis testing in (20) we assume that the secondary user terminals experience the same noise variance. While this is a very common assumption in the communications literature, geographically separated secondary user terminals may experience different noise variances due to temperature changes and/or changes in the mechanical properties they experience. In that case, the distributed hypothesis testing in (20) can be rearranged as

$$\begin{aligned} \mathcal{H}_0 &: \ \mathbf{\Sigma}_m = \sigma_m^2 \mathbf{I}_{Q_m} \quad \text{for all } m \in \{1, 2, \ldots, M\}, \\ \mathcal{H}_1 &: \ \mathbf{\Sigma}_m \succ \sigma_m^2 \mathbf{I}_{Q_m} \quad \text{for at least one } m \in \{1, 2, \ldots, M\}, \end{aligned} \tag{35}$$

where σ_m^2 is the noise variance at secondary user terminal m. The GLRT statistic for testing the above hypothesis can be obtained by following the same derivation methodology in [22, Theorem 8.3.2] which results in

$$\text{MSTS}' = \prod_{m=1}^{M} \frac{|\mathbf{R}_m|}{\left(\frac{1}{Q_m}\text{tr}(\mathbf{R}_m)\right)^{Q_m}}. \tag{36}$$

As the new global test statistic in (36) takes a form different to MSTS in (22), P_{fa} and P_{d} under unequal noise variances lead to different approximations given by

$$P_{\text{fa}} \approx 1 - \Pr[\chi^2_{\hat{f}} \leq -2\hat{\rho}\ln(\zeta)], \tag{37}$$

where $\hat{\rho} = N - \frac{\sum_{m=1}^{M} \frac{Q_m^3}{3} - \frac{K}{6} - \sum_{m=1}^{M} \frac{1}{6Q_m}}{\sum_{m=1}^{M} Q_m^2 - \sum_{m=1}^{M} Q_m - M}$, $\hat{f} = \sum_{m=1}^{M} Q_m^2 - M$ and

$$P_{\text{d}} \approx \Pr\left[\hat{Z} \leq \ln(\zeta)\right], \tag{38}$$

where $\hat{Z} \sim \mathcal{N}\left(\sum_{m=1}^{M} \mu_m, \sum_{m=1}^{M} \nu_m^2\right)$, $\mu_m = \frac{Q_m}{2}\ln(m_2') - 2Q_m \ln(m_1')$ and $\nu_m^2 = Q_m^2 \ln(m_2') - 2Q_m^2 \ln(m_1')$. The terms m_1' and m_2' are given at the top of the next page by (39) and (40), respectively, with $\sigma_m^2 < \lambda_1^m \leq \lambda_2^m \leq \ldots \leq \lambda_{Q_m}^m < \infty$ denoting the eigenvalues of $\mathbf{H}_m\mathbf{H}_m^{\dagger} + \sigma_m^2\mathbf{I}_{Q_m}$ and $\mathbf{H}_m$ denoting the $Q_m \times P$ channel matrix between the P primary users and the Q_m receive antennas at secondary user terminal m. More details on the derivation of (37) and (38) are given in Appendix B.

Fig. 5 plots P_{fa} versus the detection threshold ζ for different number of sample sizes N. Here we select an example where $P = 3$, $M = 4$, $Q_m = 2, \forall m \in \{1, 2, \ldots 4\}$ and examine $N = 50, 100$ and 200. The noise variances of the four secondary user terminals are selected as $\sigma_1^2 = 1$, $\sigma_2^2 = 2$, $\sigma_3^2 = 3$ and $\sigma_4^2 = 4$. Once again, the figure illustrates that for all three cases the approximation in (37) is very accurate. Note that the accuracy of (37) decreases for small N, since the approximation ignores higher order terms of inverse powers of N. Despite this, however, even for a small value of $N = 50$, the approximation remains tight, as witnessed in Fig. 5.

Fig. 6 plots P_{d} versus the detection threshold ζ for different number of sample sizes N. Here we select an example where $P = 3$, $M = 4$, $Q_m = 5, \forall m \in \{1, 2, \ldots 4\}$ and examine $N = 50, 100$ and 200. We fix the transmit power values to $\gamma_1 = \gamma_2 = \gamma_3 = -20$ dB. Similar to Fig. 5, the noise variances of the four secondary user terminals are selected as $\sigma_1^2 = 1$, $\sigma_2^2 = 2$, $\sigma_3^2 = 3$ and $\sigma_4^2 = 4$. The figure clearly illustrates that for all three cases the approximation in (38) is very accurate.

This article has been accepted for publication in a future issue of this journal, but has not been fully edited. Content may change prior to final publication. Citation information: DOI 10.1109/TCOMM.2018.2880902, IEEE Transactions on Communications

$$m_1' = \left(\frac{NQ_m - 1}{Q_m^2}\right) \prod_{k=1}^{Q_m} (\lambda_k^m)^{-1/Q_m} \prod_{j=0}^{Q_m-1} \frac{\Gamma(N - Q_m - 1/Q_m + 1 + j)}{\Gamma(N - Q_m + 1 + j)} \sum_{i=1}^{Q_m} \lambda_i^m, \tag{39}$$

$$m_2' = \left(\frac{NQ_m - 2}{Q_m^3}\right) \prod_{k=1}^{Q_m} (\lambda_k^m)^{-2/Q_m} \prod_{j=0}^{Q_m-1} \frac{\Gamma(N - Q_m - 2/Q_m + 1 + j)}{\Gamma(N - Q_m + 1 + j)} \left[\sum_{i=1}^{Q_m} \lambda_i^m + \left(N - \frac{2}{Q_m}\right) \left(\sum_{i=1}^{Q_m} \lambda_i^m\right)^2\right], \tag{40}$$

B. Meta Analysis

In this subsection we present the second novel distributed spectrum sensing technique named meta analysis. Meta analysis refers to the synthesis of data from multiple independent tests. Several techniques of meta analysis are available in the literature. In this paper, we use the Fisher's method which combines the results from several independent tests bearing upon the same overall hypothesis to produce a global test statistic [29].

Similar to the multisample sphericity test, under this distributed setup we can define the hypothesis $\mathcal{H}_0$ for sphericity as given in (20). Based on the measurements over the N time slots, each secondary user terminal calculates the extreme value probabilities, commonly known as p-values. The p-value at the secondary user terminal m can be written as

$$p_m = \Pr[\mathrm{TS}_m \leq \overline{\mathrm{TS}}_m | \mathcal{H}_0] \tag{41}$$

where $\mathrm{TS}_m = \frac{|\mathbf{R}_m|}{\left(\frac{1}{Q_m}\mathrm{tr}(\mathbf{R}_m)\right)^{Q_m}}$, is the random variable representing the local GLRT at the secondary user terminal m and $\overline{\mathrm{TS}}_m$ is the current value of this test statistic. It is important to note that the MSTS expression in (22) reduces to TS_m when $M = 1$. As such, we can follow the same steps as in the derivation of P_{fa} in (14) to find an analytical approximation for p_m as

$$p_m \approx 1 - \Pr[\chi^2_{f_m} \leq -2\rho_m \ln(\overline{\mathrm{TS}}_m)], \tag{42}$$

where $f_m = Q_m^2 - 1$, $\rho_m = N - \frac{1+Q_m^2-2Q_m^4}{6Q_m(1-Q_m^2)}$.

Having computed the p-value, each secondary user terminal sends it to the central processor. Thus, instead of sending the whole matrix $\mathbf{X_m}$, which is the case with the centralized spectrum sensing, meta analysis requires each secondary user terminal to send a single real number. The central processor collects all the p-values from the M secondary user terminals and combines them according to Fisher's method to produce a global test statistic [29]

$$\mathrm{MATS} = -2 \sum_{m=1}^{M} \ln(p_m). \tag{43}$$

We determine $\mathcal{H}_0$ or $\mathcal{H}_1$ in the meta analysis test as

$$\mathrm{MATS} \underset{\mathcal{H}_1}{\overset{\mathcal{H}_0}{\lessgtr}} \zeta, \tag{44}$$

where we reject the null hypothesis if MATS is larger than the threshold ζ and reject the alternative hypothesis if MATS is smaller than ζ. In order to analyse the performance of the meta analysis sphericity test, we now proceed to derive analytical expressions for P_{fa} based on (44). We would like to note that, due to the complexity of the derivation, we are unable to derive an analytical expression for P_{d} under meta analysis.

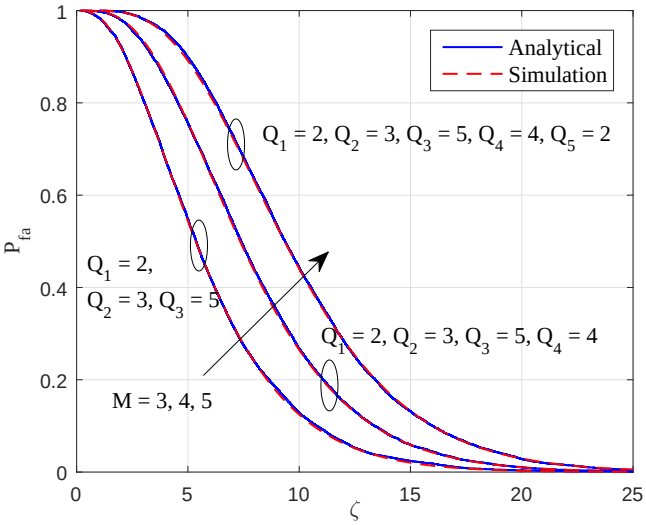

Fig. 7. Probability of false alarm vs the detection threshold for meta analysis when M = 3, 4 and 5.

1) Probability of false alarm: While the CDF of the test statistic in (43) is commonly available in the meta analysis literature [29], for the sake of completeness we summarize the derivation of P_{fa} in the following. As the test statistic MATS is a sum of the logarithms of p-values, in order to derive the CDF of MATS we first focus on the CDF of $-\ln(p_m)$. Following [29] we use the inverse transform method and write

$$\overline{\mathrm{TS}}_m = F^{-1}_{\mathrm{TS}_m,\mathcal{H}_0}(u), \tag{45}$$

where $F_{\mathrm{TS}_m,\mathcal{H}_0}$ is the CDF of TS_m under the hypothesis $\mathcal{H}_0$ and u is uniformly distributed between 0 and 1. Based on (45) we can express the p-value in (41) as $p_m = F_{\mathrm{TS}_m,\mathcal{H}_0}(F^{-1}_{\mathrm{TS}_m,\mathcal{H}_0}(u)) = u$. Hence, p_m is also uniformly distributed between 0 and 1 and the CDF of $-\ln(p_m)$ has an exponential distribution. As the sum of M independent and exponentially distributed random variables has a standard chi-squared distribution with $2M$ degrees of freedom, we derive the CDF of MATS as

$$\Pr[\mathrm{MATS} \leq x] = \Pr[\chi^2_{2M} \leq x]. \tag{46}$$

Thus, the exact closed-form expression for P_{fa} in meta analysis can be derived as

$$P_{\mathrm{fa}} = 1 - \Pr[\chi^2_{2M} \leq \zeta]. \tag{47}$$

This article has been accepted for publication in a future issue of this journal, but has not been fully edited. Content may change prior to final publication. Citation information: DOI 10.1109/TCOMM.2018.2880902, IEEE Transactions on Communications

From (47) we learn that P_{fa} for meta analysis only depends on M and ζ, i.e., unlike in (14) for the multisample sphericity test, it is not a function of the sensing duration N nor the number of secondary user antennas Q_m. In the following, we use numerical examples to illustrate the accuracy of (47).

While in this paper we consider only the GLRT statistic to calculate the p-values, it is important to note that meta analysis can be implemented with secondary user terminals operating with different test statistics. For example, the approach can be used when one secondary user terminal uses the GLRT statistic and another uses a simple power detector.

Fig. 7 plots the meta analysis P_{fa} versus the detection threshold ζ for different numbers of secondary user terminals, specifically $M = 3, 4$ and 5. In each case the secondary user terminals are allocated unequal number of antennas as noted in the figure. The observation window is $N = 200$. We note that the parameters Q_m and N do not effect the P_{fa} in meta analysis. This is because under the null hypothesis the p-values have a uniform distribution that varies between zero and one. The distribution of these tail probabilities do not change with Q_m and N. Once again, the results obtained using the analytical expression in (47) agree closely with the Monte-Carlo simulations. Note that while the probability of false alarm expression is exact, the p-values used to compute MATS use the chi-squared approximation in (42), which is the cause of the slight discrepancy between the simulated and analytical results.

C. Binary Fusion

In this subsection we present the third distributed spectrum sensing technique named binary fusion. In binary fusion each secondary user terminal performs a GLRT based on its own measurements and makes a binary decision about the presence of primary users. Based on (6), the individual test statistic of secondary user terminal m is given by $\text{TS}_m = \frac{|\mathbf{R}_m|}{\left(\frac{1}{Q_m}\text{tr}(\mathbf{R}_m)\right)^{Q_m}}$. To determine $\mathcal{H}_0$ or $\mathcal{H}_1$ at each secondary user terminal admits

$$\text{TS}_m \underset{\mathcal{H}_1}{\overset{\mathcal{H}_0}{\gtrless}} \zeta. \tag{48}$$

Each secondary user terminal then sends its binary decisions to the central processor. As such, instead of sending the whole matrix $\mathbf{X}_m$, in binary fusion the secondary user terminal m sends only one bit of information. The central processor collects all M decisions and performs a binary AND or OR operation to form the final decision.

1) Probability of false alarm: If the binary AND operation is used, the central processor declares $\mathcal{H}_0$ if at least one secondary user terminal has declared $\mathcal{H}_0$. In other words, the central processor declares $\mathcal{H}_1$ if and only if all the secondary user terminals declared $\mathcal{H}_1$. As such, we can derive P_{fa} as

$$P_{\text{fa}} = \prod_{m=1}^{M} \Pr[\text{TS}_{m\mathcal{H}_0} < \zeta]. \tag{49}$$

Based on (14) we can derive an analytical approximation for P_{fa} in (49) as

$$P_{\text{fa}} \approx \prod_{m=1}^{M} [1 - \Pr[\chi^2_{f_m} \leq -2\rho_m \ln(\zeta)]], \tag{50}$$

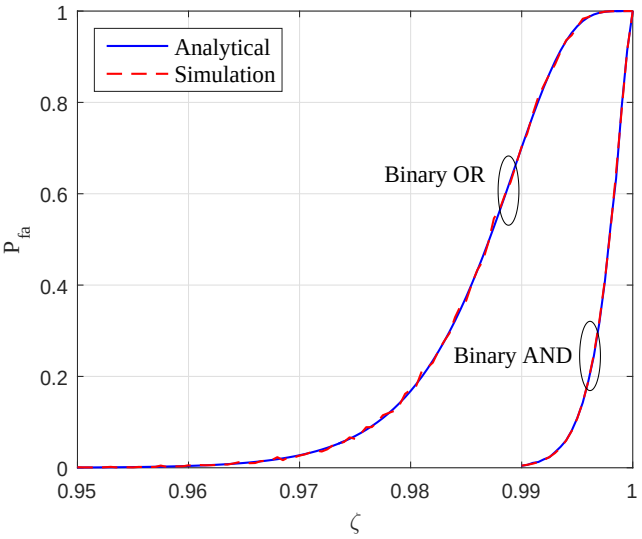

Fig. 8. Probability of false alarm vs the detection threshold for binary fusion with N = 200, $M = 4$ and $Q_m = 2$.

where $f_m = Q_m^2 - 1$, $\rho_m = N - \frac{1+Q_m^2-2Q_m^4}{6Q_m(1-Q_m^2)}$.

Similarly, if the binary OR operation is used, the central processor declares $\mathcal{H}_0$ if and only if all M secondary user terminals have declared $\mathcal{H}_0$. In other words, the central processor declares $\mathcal{H}_1$ if at least one secondary user terminal has declared $\mathcal{H}_1$. Assuming independence of test statistics formed by each secondary user terminal, the overall P_{fa} is given by

$$P_{\text{fa}} = 1 - \prod_{m=1}^{M} [1 - \Pr[\text{TS}_{m\mathcal{H}_0} < \zeta]]. \tag{51}$$

Based on (14) we can derive an analytical approximation for P_{fa} in (51) as

$$P_{\text{fa}} \approx 1 - \prod_{m=1}^{M} \Pr[\chi^2_{f_m} \leq -2\rho_m \ln(\zeta)]. \tag{52}$$

Fig. 8 plots P_{fa} versus the detection threshold ζ for both binary AND and OR fusion techniques. Here we select an example where $M = 4$, $Q_m = 2, \forall m \in \{1, 2, \ldots 4\}$ and $N = 200$. The figure clearly illustrates that the approximations in (50) and (52) very tightly follow the Monte-Carlo simulation of binary AND and OR, respectively. The figure also illustrates that for a given detection threshold the P_{fa} of binary OR fusion is higher than that of binary AND fusion.

2) Probability of detection: If the binary AND operation is used, the central processor declares $\mathcal{H}_1$ only if all M secondary user terminals have declared $\mathcal{H}_1$. Therefore, similar to the derivation of the false alarm probability, assuming independence of test statistics formed by each secondary user terminal, the overall P_{d} is written as

$$P_{\text{d}} = \prod_{m=1}^{M} \Pr[\text{TS}_{m\mathcal{H}_1} < \zeta]. \tag{53}$$

This article has been accepted for publication in a future issue of this journal, but has not been fully edited. Content may change prior to final publication. Citation information: DOI 10.1109/TCOMM.2018.2880902, IEEE Transactions on Communications

Based on (19) we can derive an analytical approximation for $P_{\rm d}$ in (53) as

$$P_{\rm d} \approx \prod_{m=1}^{M} \Pr[Z_m \leq \ln(\zeta)], \tag{54}$$

where $Z_m \sim \mathcal{N}(\mu_m, \nu_m^2)$.

Similarly, if the binary OR operation is used, the central processor declares $\mathcal{H}_1$ if at least one secondary user terminal has declared $\mathcal{H}_1$. As such, we can derive $P_{\rm d}$ as

$$P_{\rm d} = 1 - \prod_{m=1}^{M} \left[1 - \Pr[\mathrm{TS}_{m\mathcal{H}_1} < \zeta]\right]. \tag{55}$$

Based on (19) we can derive an analytical approximation for $P_{\rm d}$ in (55) as

$$P_{\rm d} \approx 1 - \prod_{m=1}^{M} \left[1 - \Pr[Z_m \leq \ln(\zeta)]\right]. \tag{56}$$

Whilst not shown here, due to page page limitation, based on numerical results we observe that the the approximation in (56) accurately follows the Monte-Carlo simulation of binary OR fusion. The approximation in (54) is slightly loose in the upper tail regime, where P_d is close to one.

D. Comparison

In this subsection we investigate the performance of distributed spectrum sensing schemes, by comparing the ROC curves of multisample sphericity test, meta analysis, binary fusion OR and binary fusion AND. In generating the ROC curves we use our analytical approximations for $P_{\rm fa}$ and $P_{\rm d}$, that was derived in Section III. For meta analysis the $P_{\rm d}$ performance is generated using Monte-Carlo simulations. It is important to note that our accurate analytical approximations save a significant amount of run time when compared to the Monte-Carlo simulations.

It is important to note that the amount of information exchanged between the central processor and the secondary user terminals are different in each distributed sensing technique. In the multisample sphericity test each secondary user terminal exchanges two real numbers with the central processor, while in meta analysis this amount is halved. In binary fusion, the amount of information exchanged is further reduced to a single binary data bit per secondary user terminal.

Fig. 9 plots $P_{\rm d}$ versus $P_{\rm fa}$ for the four distributed sensing schemes analyzed in this section. The $P_{\rm fa}$ approximations for the multisample sphericity test, meta analysis, binary fusion AND and binary fusion OR are generated using (27), (47), (50) and (52), respectively. The $P_{\rm d}$ approximations for the multisample sphericity test, binary fusion AND and binary fusion OR are generated using (34), (54) and (56), respectively. We fix $M = 2$, $Q_1 = Q_2 = 3$, $P = 2$ and examine $N = 50, 100$. The noise variance $\sigma^2 = 1$ and $\gamma_1 = \gamma_2 = -10$ dB.

As expected, binary OR and binary AND fusion perform worse than the other two, with binary OR fusion considerably outperforming binary AND fusion. Importantly, we observe a very small performance difference between that of the multisample sphericity test and meta analysis. This represents

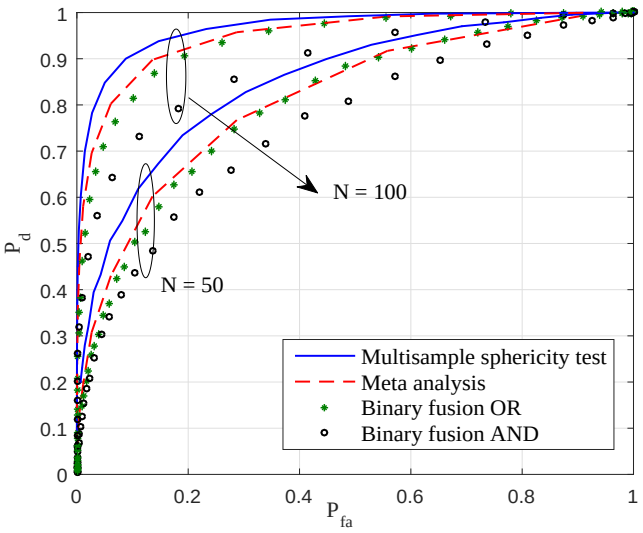

Fig. 9. Probability of detection vs the probability of false alarm for distributed spectrum sensing, when $M = 2$, $Q_m = 3$, $P = 2$ and $N = 50, 100$.

a promising result, as the meta analysis approach halves the feedback overhead of the multisample approach (one real number per secondary terminal versus two real numbers). In the tail regime, the performance of all four techniques seems to coincide in the linear scale presented in Fig. 9. In the log scale, we can observe that the performance the multisample sphericity test and meta analysis outperforms binary fusion even in the lower tail regime. For example, when $N = 50$ and $\zeta = 0.01$, i.e., in the lower tail regime, the P_d values of the multisample sphericity test, meta analysis, binary fusion OR and AND take 0.65, 0.56, 0.46 and 0.37, respectively. In the upper tail regime, however, all the techniques seems to have similar performance, with only binary fusion AND performing worse than the other three. It is also important to note that the plots in Fig. 9 were generated for one random instance of channel values. The performance of all four techniques vary when we change the channel values. However, we observe the same pattern in all channel instances.

IV. Conclusion

Multiple-antenna signal detection has been investigated in cognitive radio networks with arbitrary number of primary and secondary users. Based on the sphericity test, we analyze the performance of centralized and decentralized spectrum sensing. In centralized spectrum sensing, all raw data available at the secondary users are combined in signal detection while in decentralized spectrum sensing only partial data needs to be sent to a central processor. We propose two novel distributed spectrum sensing techniques, namely, the multisample sphericity test and meta analysis. In the multisample sphericity test each secondary user terminal sends only two real numbers, and in meta analysis they send only one real number to the central processor. Thus the amount of data shared between secondary users and the central processor is much less when compared to the centralized spectrum sensing, allowing the

This article has been accepted for publication in a future issue of this journal, but has not been fully edited. Content may change prior to final publication. Citation information: DOI 10.1109/TCOMM.2018.2880902, IEEE Transactions on Communications

application of these distributed spectrum sensing techniques to larger cognitive radio networks. We have derived easy-to-compute and accurate analytical expressions for the false alarm and the detection probabilities. Furthermore, we analyze the performance of two simple fusion techniques based on binary AND and binary OR combining and provide accurate approximations for the false alarm and the detection probabilities. Extensive numerical examples are used to illustrate the accuracy of our approximations. ROC curves are presented to compare the performance of the proposed methods.

APPENDIX A
DISTRIBUTION OF TS UNDER $\mathcal{H}_1$

Here we present the proof of (16). As described in II-B2, we are motivated to approximate the distribution of $\ln(\text{TS}_{\mathcal{H}_1})$ using a Gaussian distribution with mean μ and variance ν^2. Let us first define a new random variable X such that

$$X \approx \ln\left(\left(\frac{1}{\text{TS}_{\mathcal{H}_1}}\right)^{1/K}\right), \tag{57}$$

and $X \sim \mathcal{N}(-\mu/K, \nu^2/K^2)$. Based on (57), we can approximate the first and the second moments of $(\text{TS}_{\mathcal{H}_1})^{-1/K}$ as

$$m_1 \approx e^{-\frac{\mu}{K}+\frac{\nu^2}{2K^2}}, \tag{58}$$

$$m_2 \approx e^{-\frac{2\mu}{K}+\frac{2\nu^2}{K^2}}, \tag{59}$$

where (58) and (59) are derived using the moment generating function. Next, we take the ratio between (58) and (59) and do some mathematical manipulations to derive approximate expressions for μ and ν^2 in-terms m_1 and m_2 as

$$\mu \approx \frac{K}{2}\ln(m_2) - 2K\ln(m_1), \tag{60}$$

$$\nu^2 \approx K^2\ln(m_2) - 2K^2\ln(m_1). \tag{61}$$

The exact expressions for the moments of $(\text{TS}_{\mathcal{H}_1})^{-1/K}$ can be derived using [20, eq. (8)] which results in (60) and (61) for m_1 and m_2, respectively. Thus, the CDF Of $\ln(\text{TS}_{\mathcal{H}_1})$ can be approximated by

$$\text{Pr}[\ln(\text{TS}_{\mathcal{H}_1}) \leq x] \approx \text{Pr}[Z \leq x], \tag{62}$$

where $Z \sim \mathcal{N}(\mu, \nu^2)$. The expression in (62) can be rearranged as (16), completing the proof.

APPENDIX B
DERIVATION OF (37) AND (38)

Here we present a detailed derivation of (37) and (38). Let us denote the random variable representing the local GLRT at the secondary user terminal m by $\text{TS}_m = \frac{|\mathbf{R}_m|}{\left(\frac{1}{Q_m}\text{tr}(\mathbf{R}_m)\right)^{Q_m}}$. The terms $\text{TS}_{m\mathcal{H}_0}$ and $\text{TS}_{m\mathcal{H}_1}$ denote TS_m under the null hypothesis and the non-null hypothesis, respectively. It is straightforward to derive the exact n-th moment of the N-th power of $\text{TS}_{m\mathcal{H}_0}$ by simply replacing K in (24) by Q_m. Noting that $\text{MSTS}' = \prod_{m=1}^{M}\text{TS}_m$, the n-th moment of the N-th power of MSTS' under the null hypothesis can then be derived as

$$\text{E}[(\text{MSTS}'_{\mathcal{H}_0})^{Nn}] = \prod_{m=1}^{M}\frac{Q_m^{nNQ_m}\Gamma(NQ_m)}{\Gamma(NQ_m+nNQ_m)}\prod_{q=1}^{Q_m}\frac{\Gamma(N+nN+1-q)}{\Gamma(N+1-q)}, \tag{63}$$

where $\text{MSTS}'_{\mathcal{H}_0}$ denotes MSTS' under $\mathcal{H}_0$. Similar to the equal noise case, next we proceed to compare (63) with [24, Section 8.5.1, eq. (1)]. We observe that the expression in [24, Section 8.5.1, eq. (1)] reduces to (63) when the constant $K = \prod_{m=1}^{M}\Gamma(NQ_m)\left(\prod_{m=1}^{M}\prod_{q=1}^{Q_m}\Gamma(N+1-q)\right)^{-1}$, $b = M$, $a = K$, $y_j = NQ_j$, $x_k = N\ \forall\ k \in \{1,2,\ldots,a\}$, $\eta_j = 0$ and $\{-\xi_1,-\xi_2,\ldots,-\xi_a\} = \{0,\ldots,Q_1-1,0,\ldots,Q_2-1,\ldots,0,\ldots,Q_M-1\}$. Thus, we follow the expansion method in [24, Section 8.5.1] and derive an approximation to the CDF of $-2\hat{\rho}\ln(\text{MSTS}'_{\mathcal{H}_0})$ as

$$\text{Pr}[-2\hat{\rho}\ln(\text{MSTS}'_{\mathcal{H}_0}) \leq x] \approx \text{Pr}[\chi^2_{\hat{f}} \leq x], \tag{64}$$

which results in (37) for the false alarm probability of multisample sphericity test under unequal noise variances.

Under the non-null hypothesis, we use the result in (16) to first approximate the distribution of $\ln\left(\text{TS}_{m\mathcal{H}_1}\right)$ using a Gaussian distribution with mean μ_m and variance ν_m^2. Let us first define a new random variable X_m such that $X_m \sim \mathcal{N}(-\mu_m/Q_m, \nu_m^2/Q_m^2)$ and

$$X_m \approx \ln\left(\left(\frac{1}{\text{TS}_{m\mathcal{H}_1}}\right)^{1/Q_m}\right). \tag{65}$$

Based on (65), we can approximate the first and the second moments of $\left(\text{TS}_{m\mathcal{H}_1}\right)^{-1/Q_m}$ as

$$m'_1 \approx e^{-\frac{\mu_m}{Q_m}+\frac{\nu_m^2}{2Q_m^2}}, \tag{66}$$

$$m'_2 \approx e^{-\frac{2\mu_m}{Q_m}+\frac{2\nu_m^2}{Q_m^2}}, \tag{67}$$

where (66) and (67) are derived using the moment generating function. Next, we take the ratio between (66) and (67) and do some mathematical manipulations to derive approximate expressions for μ_m and ν_m^2 in-terms m'_1 and m'_2 as

$$\mu_m \approx \frac{Q_m}{2}\ln(m'_2) - 2Q_m\ln(m'_1), \tag{68}$$

$$\nu_m^2 \approx Q_m^2\ln(m'_2) - 2Q_m^2\ln(m'_1). \tag{69}$$

The exact expressions for the moments of $\left(\text{TS}_{m\mathcal{H}_1}\right)^{-1/Q_m}$ can be derived using [20, eq. (8)] which results in (39) and (40) for m'_1 and m'_2, respectively. Since $\text{MSTS}' = \prod_{m=1}^{M}\text{TS}_m$, we can finally approximate the distribution of $\ln\left(\text{MSTS}'\right)$ using a Gaussian distribution with mean $\sum_{m=1}^{M}\mu_m$ and variance $\sum_{m=1}^{M}\nu_m^2$ and write

$$\text{Pr}[\text{MSTS}'_{\mathcal{H}_1} \leq x] \approx \text{Pr}\left[\hat{Z} \leq \ln(x)\right], \tag{70}$$

where here $\hat{Z} \sim \mathcal{N}\left(\sum_{m=1}^{M}\mu_m, \sum_{m=1}^{M}\nu_m^2\right)$, $\mu_m = \frac{Q_m}{2}\ln(m'_2) - 2Q_m\ln(m'_1)$. This results in (38) for the detection probability of multisample sphericity test under unequal noise variances.

This article has been accepted for publication in a future issue of this journal, but has not been fully edited. Content may change prior to final publication. Citation information: DOI 10.1109/TCOMM.2018.2880902, IEEE Transactions on Communications

APPENDIX C
DERIVATION OF $\tilde{m_1}$ AND $\tilde{m_2}$

In this section, we derive an analytical expressions for the first and the second moments of $\frac{1}{\text{MSTS}_{\mathcal{H}_1}}$. From [18, eq. (40)], we learn that the PDF of the sample covariance matrix at the secondary user terminal m, is given by

$$f(\mathbf{R}_m) = \frac{|\mathbf{R}_m|^{N-Q_m}\Delta_{N,Q_m}\exp\left(\text{tr}(-\mathbf{\Sigma}_m^{-1}\mathbf{R}_m)\right)}{|\mathbf{\Sigma}_m|^N}, \quad (71)$$

where $\Delta_{N,Q_m} = 1/\left(\pi^{\frac{Q_m}{2}(Q_m-1)}\prod_{q=1}^{Q_m-1}\Gamma(N-q)\right)$. Based on (71), we can write the r-th moment of $\frac{1}{\text{MSTS}_{\mathcal{H}_1}}$ as

$$\text{E}\left[\frac{1}{\text{MSTS}_{\mathcal{H}_1}^r}\right] = \frac{1}{K^{Kr}}\int_{\mathbf{R}_1}\cdots\int_{\mathbf{R}_M}\frac{\left(\sum_{m=1}^M \text{tr}(\mathbf{R}_m)\right)^{Kr}}{\prod_{m=1}^M|\mathbf{R}_m|^r} \times\prod_{j=1}^M\frac{|\mathbf{R}_j|^{N-Q_j}\Delta_{N,Q_j}\exp\left(\text{tr}(-\mathbf{\Sigma}_j^{-1}\mathbf{R}_j)\right)}{|\mathbf{\Sigma}_j|^N}d\mathbf{R}_1\ldots d\mathbf{R}_M. \quad (72)$$

Assuming that all the secondary user terminals have the same number of antennas, i.e., $Q_m = Q\ \forall\{1,2,\ldots,M\}$, we rearrange (72) as

$$\text{E}\left[\frac{1}{\text{MSTS}_{\mathcal{H}_1}^r}\right] = \frac{1}{K^{Kr}}\prod_{m=1}^M\frac{\Delta_{N,Q}}{|\mathbf{\Sigma}_m|^r\Delta_{N-r,Q}}\int_{\mathbf{R}_1}\cdots\int_{\mathbf{R}_M}\left(\sum_{m=1}^M\text{tr}(\mathbf{R}_m)\right)^{Kr} \times\prod_{j=1}^M\frac{|\mathbf{R}_j|^{N-Q-r}\Delta_{N-r,Q}\exp\left(\text{tr}(-\mathbf{\Sigma}_j^{-1}\mathbf{R}_j)\right)}{|\mathbf{\Sigma}_j|^{N-r}}d\mathbf{R}_1\ldots d\mathbf{R}_M. \quad (73)$$

Identifying that the M-fold integral in (73) represents the expected value of $\left(\sum_{m=1}^M\text{tr}(\mathbf{R}_m)\right)^{Kr}$, we further simplify (73) as

$$\text{E}\left[\frac{1}{\text{MSTS}_{\mathcal{H}_1}^r}\right] = \frac{1}{K^{Kr}}\left(\frac{\Delta_{N,Q}}{\Delta_{N-r,Q}}\right)^M\left[\prod_{m=1}^M\frac{1}{|\mathbf{\Sigma}_m|^r}\right] \times\text{E}\left[\left(\sum_{m=1}^M\text{tr}(\mathbf{R}_m)\right)^{Kr}\right]. \quad (74)$$

Based on (74), we next proceed to find $\tilde{m_1}$. We set $r=1$ in (74) and write

$$\tilde{m_1} = \frac{1}{K^K\prod_{j=0}^{Q-1}(N-1-j)^M\prod_{m=1}^M|\mathbf{\Sigma}_m|} \times\text{E}\left[\left(\sum_{m=1}^M\text{tr}(\mathbf{R}_m)\right)^K\right]. \quad (75)$$

Note that the derivation of the expected value of $\frac{1}{\text{MSTS}_{\mathcal{H}_1}}$ has now reduced to deriving the K-th moment of $\sum_{m=1}^M\text{tr}(\mathbf{R}_m)$. Let us denote $\omega_m = \text{tr}(\mathbf{R}_m)$. To derive the K-th moment of $\sum_{m=1}^M\omega_m$ we use the multinomial expansion and write

$$\text{E}\left[\left(\sum_{m=1}^M\omega_m\right)^K\right] = \sum_{\sum i_j=K, 0\le i_j\le K}\left(\frac{K!}{i_1!i_2!\ldots i_M!}\right)\prod_{m=1}^M\text{E}\left[\omega_m^{i_m}\right], \quad (76)$$

where the product in (76) results from the independence of ω_m. Note that $\omega_m = \sum_{i=1}^Q\frac{\lambda_i^m\chi_i}{2}$, where λ_i^m denotes the i-th eigenvalue of $\mathbf{h}_m\mathbf{h}_m^\dagger + \sigma_m^2\mathbf{I}_{Q_m}$ and χ_i denotes a random variable with the standard chi-squared distribution, with $2(N-1)$ degrees of freedom. Thus, we can express $\text{E}\left[\omega_m^{i_m}\right]$ as

$$\text{E}\left[\omega_m^{i_m}\right] = \sum_{\sum_{j_q=i_m}, 0\le j_q\le i_m}\left(\frac{i_m!}{j_1!j_2!\ldots j_Q!}\right)\frac{\prod_{q=1}^Q(\lambda_q^m)^{j_q}\text{E}\left[\chi_q^{j_q}\right]}{2^{i_m}}, \quad (77)$$

where (77) are derived by applying the multinomial expansion. Let us denote $\text{E}\left[\chi_q^{j_q}\right]$ by $\mu_{j_q}^{(2N-2)}$. The moments of a chi-squared variable is well-known and can be found in [30] as

$$\mu_q^{(2N-2)} = \frac{2^{j_q}\Gamma(j_q+N-1)}{\Gamma(N-1)}. \quad (78)$$

We substitute (78) into (77), using which (76) can be re-expressed as

$$\text{E}\left[\left(\sum_{m=1}^M\omega_m\right)^K\right] = \sum_{\sum i_j=K, 0\le i_j\le K}\left[\left(\frac{K!}{i_1!i_2!\ldots i_M!}\right)\prod_{m=1}^M\Xi_{m,i_m}\right], \quad (79)$$

where

$$\Xi_{m,i_m} = \sum_{\sum_{j_q=i_m}, 0\le j_q\le i_m}\left[\left(\frac{i_m!}{j_1!j_2!\ldots j_Q!}\right)\frac{\prod_{q=1}^Q(\lambda_q^m)^{j_q}\mu_q^{(2N-2)}}{2^{i_m}}\right]. \quad (80)$$

Substituting (79) into (75) we finally derive a closed-form expression for $\tilde{m_1}$ as

$$\tilde{m_1} = \frac{1}{K^K\prod_{j=0}^{Q-1}(N-1-j)^M\prod_{m=1}^M|\mathbf{\Sigma}_m|}\sum_{\sum i_j=K, 0\le i_j\le K} \times\left[\left(\frac{K!}{i_1!i_2!\ldots i_M!}\right)\prod_{m=1}^M\Xi_{m,i_m}\right]. \quad (81)$$

This article has been accepted for publication in a future issue of this journal, but has not been fully edited. Content may change prior to final publication. Citation information: DOI 10.1109/TCOMM.2018.2880902, IEEE Transactions on Communications

Based on (74), we next proceed to find $\tilde{m}_2$. Following a similar approach to deriving the K-th moment of $\sum_{m=1}^{M} \text{tr}(\mathbf{R}_m)$ we derive the $2K$-th moment of $\sum_{m=1}^{M} \text{tr}(\mathbf{R}_m)$ as

$$\text{E}\left[\left(\sum_{m=1}^{M} \omega_m\right)^{2K}\right] = \sum_{\sum i_j = 2K, 0 \leq i_j \leq 2K} \left[\left(\frac{(2K)!}{i_1! i_2! \ldots i_M!}\right) \prod_{m=1}^{M} \Theta_{m,i_m}\right], \quad (82)$$

where

$$\Theta_{m,i_m} = \sum_{\sum_{j_q = i_m}, 0 \leq j_q \leq i_m} \left[\left(\frac{i_m!}{j_1! j_2! \ldots j_Q!}\right) \frac{\prod_{q=1}^{Q} (\lambda_q^m)^{j_q} \mu_q^{(2N-4)}}{2^{i_m}}\right], \quad (83)$$

and $\mu_q^{(2N-4)} = \frac{2^{j_q}\Gamma(j_q+N-2)}{\Gamma(N-2)}$. Substituting (82) into (74) when $r = 2$, we derive a closed-form expression for $\tilde{m}_2$ as

$$\tilde{m}_2 = \frac{1}{\left[\prod_{j=0}^{Q-1} (N-j-1)^M (N-j-2)^M\right] \prod_{m=1}^{M} |\mathbf{\Sigma}_m|^2} \times \frac{1}{K^{2K}} \sum_{\sum i_j = 2K, 0 \leq i_j \leq 2K} \left[\left(\frac{(2K)!}{i_1! i_2! \ldots i_M!}\right) \prod_{m=1}^{M} \Theta_{m,i_m}\right]. \quad (84)$$

REFERENCES

[1] F. C. Commission, Spectrum policy task force, *Rep. ET Docket no.*, pp. 02135, Nov. 2002.

[2] B. Li, S. Li, A. Nallanathan, and C. Zhao, Deep sensing for future spectrum and location awareness 5G communications, *IEEE J. Sel. Areas Commun.*, vol. 33, pp. 13311344, Jul. 2015.

[3] S. Haykin, Cognitive radio: Brain-empowered wireless communications, *IEEE J. Sel. Areas Commun.*, vol. 23, pp. 201220, Feb. 2005.

[4] I. F. Akyildiz, W. Y. Lee, M. C. Vuran, and S. Mohanty, A survey on spectrum management in cognitive radio networks, *IEEE Commun. Mag.*, vol. 46, pp. 4048, Jan. 2008.

[5] G. Staple and K. Werbach, The end of spectrum scarcity, *IEEE Spectrum*, vol. 41, pp. 4852, Mar. 2004.

[6] D. Cabric, Addressing feasibility of cognitive radios, *IEEE Trans. Signal Process.*, vol. 25, pp. 8593, Nov. 2008.

[7] J. M. Peha, Sharing spectrum through spectrum policy reform and cognitive radio, *Proc. IEEE*, vol. 97, pp. 708719, 2009.

[8] N. I. Miridakis, T. A. Tsiftsis, G. C. Alexandropoulos, and M. Debbah, Simultaneous spectrum sensing and data reception for cognitive spatial multiplexing distributed systems, *IEEE Trans. Wireless Commun.*, vol. 16, pp. 33133327, Oct. 2017.

[9] C. Cordeiro, K. Challapali, and N. S. Shankar, IEEE 802.22: The first worldwide wireless standard based on cognitive radios, in *IEEE Int. Symp. New Frontiers Dynam. Spectrum Access Netw. (DySPAN)*, Baltimore, USA, Nov. 2005, pp. 328337.

[10] V. Kostylev, Energy detection of a signal with random amplitude, in *IEEE International Conference on Communications (ICC)*, New York, NY, USA, USA, Aug. 2002, pp. 16061610.

[11] F. Digham, M. S. Alouini, and M. K. Simon, On the energy detection of unknown signals over fading channels, in *IEEE International Conference on Communications (ICC)*, May 2003, pp. 35753579.

[12] S. Kritchman and B. Nadlerg, Non-parametric detections of the number of signals: Hypothesis testing and random matrix theory, *IEEE Trans. Signal Process.*, vol. 57, pp. 39303941, Oct. 2009.

[13] A. Taherpour, M. N. Kenari, and S. Gazor, Multiple antenna spectrum sensing in cognitive radios, *IEEE Trans. Wireless Commun.*, vol. 9, pp. 814823, Feb. 2010.

[14] Y. Zeng, C. L. Koh, and Y. C. Liang, Maximum eigenvalue detection: theory and application, in *IEEE International Conference on Communications (ICC)*, Beijing, China, May 2008.

[15] S. Haykin, D. Thomson, and J. Reed, Spectrum sensing for cognitive radio, *Proc. IEEE*, vol. 97, pp. 849877, May 2009.

[16] Y. Zeng and Y. C. Liang, Spectrum-sensing algorithms for cognitive radio based on statistical covariances, vol. 4, pp. 18041815, May 2009.

[17] R. Zhang, T. J. Lim, Y. C. Liang, and Y. Zeng, Multi-antenna based spectrum sensing for cognitive radios: A GLRT approach, *IEEE Trans. Commun.*, vol. 58, pp. 8488, Jan. 2010.

[18] L. Wei and O. Tirkkonen, Spectrum sensing in the presence of multiple primary users, *IEEE Trans. Commun.*, vol. 60, pp. 12681277, May 2012.

[19] R. H. Y. Louie, M. R. McKay, and Y. Chen, Multiple-antenna signal detection in cognitive radio networks with multiple primary user signals, in *IEEE Int. Conf. Commun. (ICC)* 2014, Sydney, Australia, Jun. 2014, pp. 49514956.

[20] D. M. Jimenez, R. H. Y. Louie, M. R. McKay, and Y. Chen, Analysis and design of multiple-antenna cognitive radios with multiple primary user signals, *IEEE Trans. Signal Process.*, vol. 63, pp. 49254939, Sep. 2015.

[21] J. W. Mauchly, Significance test for sphericity of a normal n-variate distribution, *Annals of Mathematical Statistics*, vol. 11, pp. 204209, Jan. 1940.

[22] R. J. Muirhead, *Aspects of multivariate statistical theory*. New Jersey, USA. Wiley and Sons, Inc, 1982.

[23] K. V. Mardia, J. T. Kent, and J. M. Bibby, *Multivariate Analysis*. New York, NY, USA: Academic, 1979.

[24] T. W. Anderson, *An Introduction to Multivariate Statistical Analysis*. Wiley, 2003.

[25] I. S. Gradshteyn and I. M. Ryzhik, *Table of Integrals, Series, and Products*, 7th ed. Academic Press, 2007.

[26] D. K. Nagar and A. K. Gupta, On testing multisample sphericity in the complex case, *Journal of the Korean Statistical Society*, vol. 13, pp. 7380, Jan. 1984.

[27] A. K. Gupta and D. K. Nagar, Nonnull distribution of likelihood ratio criterion for testing multisample sphericity in the complex case, *Austral. Journal of Statistics*, vol. 30, pp. 307318, Jan. 1988.

[28] P. J. Smith, R. Senanayake, P. A. Dmochowski, and J. S. Evans, Novel distributed spectrum sensing techniques for cognitive radio networks, in *IEEE Wireless Communications and Networking Conference (WCNC)*, Barcelona, Spain, Apr. 2018.

[29] R. A. Fisher, *Statistical Methods for Research Workers*, 5th ed. Tweeddale Court, Edinburgh: Oliver and Boyd, 1925.

[30] M. K. Simon, *Probability Distributions Involving Gaussian Random Variables*. New York, Springer, 2002.

Peter J. Smith (M'93-SM'01-F'15) received the B.Sc. degree in mathematics and the Ph.D. degree in statistics from the University of London, London, U.K., in 1983 and 1988, respectively. From 1983 to 1986, he was with the Telecommunications Laboratories, General Electric Company Hirst Research Centre. From 1988 to 2001, he was a Lecturer in statistics with the Victoria University of Wellington, Wellington, New Zealand. During 20012015, he was with the Department of Electrical and Computer Engineering, University of Canterbury, Christchurch, New Zealand. In 2015, he joined Victoria University of Wellington as Professor of statistics. His research interests include the statistical aspects of design, modeling, and analysis for communication systems, cognitive radio, massive multiple-inputmultiple-output, and millimeter-wave systems.

Rajitha Senanayake (S'11-M'16) received the B. E. degree in Electrical and Electronics Engineering from the University of Peradeniya, Sri Lanka, and the BIT degree in Information Technology from the University of Colombo, Sri Lanka, in 2009 and 2010, respectively. From 2009 to 2011, she was with the research and development team at Excel Technology, Sri Lanka. She received the Ph.D. degree in Electrical and Electronics Engineering from the University of Melbourne, Australia, in 2015. From 2015 to 2016 she was with the Department of Electrical and Computer Systems Engineering, Monash University, Australia. Currently she is a research fellow at the Department of Electrical and Electronics Engineering at the University of Melbourne, Australia. She is a recipient of the Australian Research Council Discovery Early Career Researcher Award. Her research interests are in cooperative communications, distributed antenna systems and Fog computing.

Pawel A. Dmochowski (S02-M07-SM'11) was born in Gdansk, Poland. He received a B.A.Sc (Engineering Physics) from the University of British Columbia, and M.Sc. and Ph.D. degrees from Queens University, Kingston, Ontario. He is currently with the School of Engineering and Computer Science at Victoria University of Wellington, New Zealand. Prior to joining Victoria University of Wellington, he was a Natural Sciences and Engineering Research Council (NSERC) Visiting Fellow at the Communications Research Centre Canada. In 2014-2015 he was a Visiting Professor at Carleton University in Ottawa.

He is a Senior Member of the IEEE. Between 2014-2015 he was the Chair of the IEEE Vehicular Technology Society Chapters Committee. He has served as an Editor for IEEE Communications Letters and IEEE Wireless Communications Letters. His research interests include mmWave, Massive MIMO and Cognitive Radio systems, with a particular emphasis on statistical performance characterisation.

Jamie S. Evans (S'93-M'98) was born in Newcastle, Australia, in 1970. He received the B.S. degree in physics and the B.E. degree in computer engineering from the University of Newcastle, in 1992 and 1993, respectively, where he received the University Medal upon graduation. He received the M.S. and the Ph.D. degrees from the University of Melbourne, Australia, in 1996 and 1998, respectively, both in electrical engineering, and was awarded the Chancellor's Prize for excellence for his Ph.D. thesis. From March 1998 to June 1999, he was a Visiting Researcher in the Department of Electrical Engineering and Computer Science, University of California, Berkeley. Since returning to Australia in July 1999 he has held academic positions at the University of Sydney, the University of Melbourne and Monash University. He is currently a Professor and Deputy Dean in the Melbourne School of Engineering at the University of Melbourne. His research interests are in communications theory, information theory, and statistical signal processing with a focus on wireless communications networks.